SLAC-PUB-13234
arXiv:0805.1260v1[astro-ph]
May 2008

DRAFT VERSION MAY 9, 2008
Preprint typeset using LaTeX style emulateapj v. 3/25/03

ON THE POSSIBLE ASSOCIATION OF ULTRA HIGH ENERGY COSMIC RAYS WITH NEARBY ACTIVE GALAXIES

IGOR V. MOSKALENKO[1] AND ŁUKASZ STAWARZ[2]
Kavli Institute for Particle Astrophysics and Cosmology, Stanford University, Stanford, CA 94309

TROY A. PORTER
Santa Cruz Institute for Particle Physics, University of California, Santa Cruz, CA 95064

AND

CHI C. CHEUNG
NASA Goddard Space Flight Center, Astrophysics Science Division, Code 661, Greenbelt, MD 20771
Draft version May 9, 2008

ABSTRACT

Data collected by the Pierre Auger Obsevatory provide evidence for anisotropy in the arrival directions of cosmic rays (CRs) with energies >57 EeV that suggests a correlation with the positions of active galactic nuclei (AGN) located within ∼75 Mpc. However, this analysis does not take into account AGN morphology. A detailed study of the sample of AGN whose positions correlate with the CR events shows that most of them are classified as Seyfert 2 and low-ionization nuclear emission-line region (LINER) galaxies which do not differ from other local AGN of the same types. Therefore, the claimed correlation between the CR events observed by the Pierre Auger Observatory and local active galaxies should be considered as resulting from a chance coincidence, if the production of the highest energy CRs is not episodic in nature, but operates in a single object on long ($\geq$ Myr) timescales. Additionally, most of the selected sources do not show significant jet activity, and hence – in the framework of the jet paradigm – there are no reasons for expecting them to accelerate CRs up to the highest energies, $\sim 10^{20}$ eV, at all. If the extragalactic magnetic fields and the sources of these CRs are coupled with matter, it is possible that the deflection angle is larger than expected in the case of a uniform source distribution due to effectively larger fields. A future analysis has to take into account AGN morphology and may yield a correlation with a larger deflection angle and/or more distant sources. We further argue that Cen A alone could be associated with at least 4 events due to its large radio extent, and Cen B can be associated with more than 1 event due to its proximity to the Galactic plane and, correspondingly, the stronger Galactic magnetic field the ultra high energy CRs (UHECRs) encounter during propagation. If the UHECRs associated with these events are indeed accelerated by Cen A and Cen B, their deflection angles may provide information on the structure of the magnetic field in the direction of these putative sources. Future γ-ray observations (by, e.g., *Gamma-Ray Large Area Space Telescope* [GLAST], *High Energy Stereoscopic System* [HESS]) may provide additional clues to the nature of the accelerators of the UHECRs in the local Universe.

Subject headings: cosmic rays — galaxies: active — galaxies: individual (Cen A, Cen B, PKS 2158–380, PKS 2201+044) — intergalactic medium

1. INTRODUCTION

The spectrum, origin, and composition of CRs at the highest energies ($\geq 10^{18}$ eV $\equiv$ 1 EeV; hereafter UHECRs) has been a puzzle since their discovery almost 50 years ago (for a review see Nagano & Watson 2000). The isotropy of the arrival directions of UHECRs above 10^{18} eV suggests an extragalactic origin, though Galactic objects such as fast rotating neutron stars with ultrastrong magnetic fields are capable of accelerating particles up to $\sim 10^{20}$ eV (Hillas 1984). The UHECR energy losses due to photopion production on the cosmic microwave background (CMB) – the so-called GZK effect (Greisen 1966; Zatsepin & Kuz'min 1966) – mean that the sources of the highest energy particles should be cosmologically close, within ∼100 Mpc. However, observations of the spectrum at these high energies are extremely challenging due to the low overall event rate[3]. Fine structure in the CR spectrum above 10^{18} eV has been predicted (e.g., Berezinsky et al. 2006): the GZK cutoff, a pile-up bump, and a dip due to photoproduction of pairs, and indeed found in experiments, but the interpretation is not straightforward due to the large uncertainty in the source distribution, their injection spectrum, and CR chemical composition.

There are quite a few extragalactic objects capable of accelerating UHECRs. Among those are shocks from the epoch of the large scale structure formation, γ-ray bursts, galaxy clusters, AGN, in particular, those AGN with powerful jets, and the lobes of giant radio galaxies (Stanev 2007a); various exotic top-down scenarios have also been discussed but seem unlikely (e.g., Abraham et al. 2007a, 2008b). Extragalactic jets and their extended radio lobes have been proposed as one of the most likely acceleration sites of UHECRs (e.g., Biermann & Strittmatter 1987; Dermer 2007; Ostrowski 2002, and references therein). However, not all AGN have jets, and for those that do the jet properties may differ substantially between different classes/types.

There are also quite a few "known unknowns" which affect the distribution of the arrival directions of UHECRs and make

[1] Also Hansen Experimental Physics Laboratory, Stanford University, Stanford, CA 94305
[2] Also Astronomical Observatory, Jagiellonian University, ul. Orla 171, 30-244 Kraków, Poland
[3] 1 per km^2 per century at $\sim 10^{20}$ eV

Submitted to Astrophysical Journal

Work supported in part by US Department of Energy contract DE-AC02-76SF00515

the association with particular classes of objects a non-trivial task. Among these are the source distribution, the structure of extragalactic and Galactic magnetic fields, the nature of sources (transient vs. steady), and the energy spectrum and chemical composition at injection.

The Pierre Auger Collaboration have reported significant evidence for anisotropy in the arrival directions of UHECRs (Abraham et al. 2007a, 2008a). The anisotropy signal suggests a correlation of the events with AGN listed in the Véron-Cetty & Véron (2006) catalog with distances less than ∼100 Mpc, though other sources with a similar distribution are not ruled out[4]. The maximum correlation was found for AGN with redshift $z \leq 0.017$ (corresponding distance $D \leq 71$ Mpc), angular separation $\leq 3.2°$, and events with energy above ∼57 EeV. The list of events with energy in excess of 57 EeV consists of 27 events, and 20 of these correlate with the AGN from Véron-Cetty & Véron (2006) catalog.

In this paper we discuss the possible association between UHECRs and AGN based on a detailed analysis of a selected sample of nearby active galaxies contained within the $3.2°$ search radius of the UHECR events detected by the Pierre Auger Collaboration, drawn from the Véron-Cetty & Véron (2006) catalog, with additional AGN taken from the NASA/IPAC Extragalactic Database (NED). The AGN sample, described here in detail, consists predominantly of low-luminosity sources such as Seyfert galaxies and LINERs, and a handful of radio galaxies.

2. PHENOMENOLOGY OF LOCAL AGN

A number of weak AGN in the local Universe can be observed and even resolved due to their proximity which allows a broad range of AGN activity to be studied, while only bright ones can be seen at large distances.

Supermassive black holes ($\mathcal{M}_{\rm BH} \sim 10^6\mathcal{M}_\odot - 10^9\mathcal{M}_\odot$) are found in a number of galaxies, and there is a growing concensus that all galaxies contain accreting black holes at their centers. If the emission of the accreting/circumnuclear matter is pronounced, the galaxy is classified as active. Such emission includes a non-stellar blue continuum due to the accretion disk and strong, but narrow, forbidden emission lines resulting from photoionization of the surrounding gas by the disk radiation. It was shown recently that about 85% of all galaxies (and, in particular, almost all nearby late-type galaxies) possess detectable emission-line nuclei, which therefore could be classified as AGN. In most cases, however, the nuclear luminosity is very weak relative to the stellar radiative output of the host galaxy[5]. These nearby low-luminosity AGN can be divided into Seyfert galaxies ($\gtrsim 10\%$ of local AGN) and LINERs ($\sim 60\%$), depending on the ionization level and intensity of the emission lines[6]. For more details we refer the reader to the recent review by Ho (2008).

The rest of the local AGN assemblage is populated by radio galaxies (mostly low-power ones of the FR I type; Fanaroff & Riley 1974) and BL Lacertae objects (BL Lacs). In these sources, the radiative output of the accreting/circumnuclear gas (which may, spectroscopically, resemble closely the Seyfert or LINER types) is dominated, or at least substantially modified, by a broad-band non-thermal emission produced by relativistic jets emanating from the active centers. Also, it should be mentioned that radio galaxies and BL Lacs are hosted almost exclusively by giant elliptical and S0 galaxies, while the majority of Seyferts and LINERs ($\gtrsim 90\%$) are associated with spiral galaxies.

Some fraction of AGN exhibit in addition broad permitted emission lines (FWHM $\sim 10^3 - 10^4$ km s^{-1}) in their spectra; the presence/absence of such lines divides further the AGN population into type 1/type 2 classes. In the framework of the "AGN unification scheme", these two classes are intrinsically identical, and differ only in orientation of the accretion disk symmetry axis to the line of sight (Antonucci 1993). Namely, type 1 AGN are believed to be observed at small inclination angles (roughly $<40°$), while type 2 AGN are believed to be viewed at larger angles through a high-column-density gas and dust concentrated at pc-scale distances from the active center in a torus-like structure (co-planar with the inner accretion disks). As a result, the disk continuum and broad emission lines produced very close to supermassive black holes are heavily obscured in type 2 AGN, but not in type 1 sources. The narrow line emission, originating at larger distances ($>$ pc) from the active center, is not subjected to strong obscuration.

Such a unifying picture is supported by several observational findings, including detections of strong mid-infrared (MIR) emission due to the dusty obscuring tori in basically all different classes and types of AGN. In addition to the MIR/optical/UV non-stellar nuclear radiation, Seyferts and LINERs show characteristic X-ray emission extending from 0.1 keV up to 100 keV photon energies with photon indices $\Gamma_X \lesssim 2.0$, believed to be produced within the hot coronae of the accretion disks (see, e.g., Svensson 1996; Zdziarski 1999). The low-energy (< 2 keV) segment of this continuum is typically obscured in type 2 sources, which agrees with the unification scheme. We also note that in the framework of the unification paradigm, all BL Lacs are expected to be simply low-luminosity radio galaxies (FR Is) viewed at very small viewing angles ($\lesssim 10°$) to the jet axis.

Acceleration of particles (both electrons and protons) to ultrarelativistic energies in AGN is supposed to take place almost exclusively in collimated fast jets, which are produced (at least in some cases) by the active black hole/accretion disk systems[7]. The strong magnetization, extremely low density, non-stationary relativistic and supersonic flow pattern, and finally turbulent character of such jets (see, e.g., a review by Begelman et al. 1984), is expected to result in the formation of non-thermal particle energy distributions extending up to the highest accessible energies. Indeed, the very high energy γ-ray emission detected from blazars[8], demonstrates the ability of the nuclear (sub-pc scale) relativistic AGN outflows to efficiently accelerate electrons up to $1 - 100$ TeV energies (e.g., Celotti & Ghisellini 2008). In the case of large (kpc)-scale jets, as observed in powerful radio galaxies and radio-loud quasars, it has been speculated that proton energies in

[4] Note that the Pierre Auger Collaboration acknowledges the incompleteness of the catalog and does not make any serious claims concerning source classes.

[5] If the nuclear emission outshine the starlight of the host galaxy, the source is classified as quasar.

[6] We note that the starburst nuclei of many galaxies, as well as their H II regions, also possess ionization lines, which are however weaker than the ones observed in Seyferts or LINERs, and which are photoionized exclusively by the starburst activity.

[7] Note, that there is no observational evidence for a significant population of non-thermal particles in AGN accretion disks and disk coronae. In fact, hard X-ray/soft γ-ray emission observed from Seyferts is best modeled assuming a thermal population of electrons, albeit characterized by high temperatures of the order of 100 keV.

[8] Blazar class includes BL Lacertae objects and radio loud quasars with flat spectrum radio cores.

the range $10 - 100$ EeV range can be reached as well (e.g., Lyutikov & Ouyed 2007; Ostrowski 1998).

Not all AGN are jetted. Also, it seems that only some fraction of nuclear jets can remain relativistic and well-collimated during the propagation through the dense environments of the central parts of host galaxies. These issues are particularly relevant for Seyferts and LINERs, which differ substantially from the bona fide jet sources like radio galaxies and radio-loud quasars, lacking in particular well-defined large-scale jet structures. We also note in this context, that no galaxy classified as Seyfert or LINER has been detected so far at γ-ray energies[9].

Jet activity always manifests itself as non-thermal synchrotron radio emission produced by ultrarelativistic jet electrons. Hence, investigation of jet properties are usually addressed by detailed radio studies. In the case of local AGN, like Seyferts and LINERs, such studies are hampered due to the low luminosities and small sizes of the radio structures. Additionally, most of these sources, and in principle all local spiral-hosted AGN, show intense star formation activity (especially pronounced in the far-infrared [FIR]). Such activity is known for producing the radio-emitting outflows due to starburst-driven superwinds which, although completely different in origin, may in some (morphological and spectral) respects resemble closely jet-related activity. Thus, care must be taken when making any statement regarding jet properties in these objects with limited radio data.

What do we know about radio activity in local Seyferts and LINERs in general? Radio surveys of such AGN reveal typically complex, multi-component radio structures, consisting of compact unresolved or slightly resolved cores (detected at centimeter wavelengths in most of these objects), linear jet-like features (observed in $\sim 30\%$ of the local low-luminosity AGN), and spherical or elongated diffuse halos/radio bubbles (present in, again, $\sim 30\% - 50\%$ of the Seyfert and LINER population; e.g., Baum et al. 1993; Colbert et al. 1996; Gallimore et al. 2006; Ho & Ulvestad 2001; Morganti et al. 1999; Rush et al. 1996; Ulvestad & Wilson 1989). The total radio powers of these objects at centimeter wavelengths are in the range $\sim 10^{35} - 10^{42}$ erg s^{-1} (with median value $L_{5\mathrm{GHz}} \sim 2 \times 10^{37}$ erg s^{-1}; Ho & Ulvestad 2001), which are typically slightly higher than the total radio luminosities of "regular" spiral galaxies.

For the compact cores of Seyfert and LINERs, previously no dependence in radio power or spectral properties on the AGN type (type 1 vs. type 2) or host galaxy morphology (ellipticals vs. spirals) was found (Morganti et al. 1999; Nagar et al. 1999; Rush et al. 1996; Ulvestad & Wilson 1989). However, more recently it has been suggested that the small fraction of those Seyferts which are elliptical-hosted, and possibly also type 1 Seyferts, are characterized by relatively stronger nuclear radio activity (Nagar et al. 2005; Thean et al. 2001; Ulvestad & Ho 2001). Nevertheless, it is established that flat-spectrum radio cores can be present in all types of local low-luminosity AGN, and therefore (unlike in the case of radio galaxies and quasars) cannot be used as a good proxy for the source inclination.

It has been speculated that the flat-spectrum radio cores of Seyferts may not be due to jet activity, but rather some other processes like a nuclear starburst, or the emission of the accretion disks/obscuring tori themselves (e.g., Gallimore et al. 1997). However, the relatively high brightness temperatures of the Seyfert radio cores, 10^7 K $< T_{\mathrm{b}} < 10^9$ K, points to a synchrotron (and therefore jet-related) origin of the radio emission (Middelberg et al. 2004; Mundell et al. 2000; Nagar et al. 2005). This is supported by the excess radio emission of the local low-luminosity AGN with detected radio cores over the radio–FIR correlation established for regular spirals and starforming galaxies (Ho & Ulvestad 2001; Roy et al. 1998) which is expected to hold if the radio emission is exclusively/predominantly due to starforming activity (Condon et al. 2002; Helou et al. 1985). Also, recently found scaling relations between the nuclear radio emission of Seyferts and LINERs and their accretion power (approximated by either the $2 - 10$ keV luminosity of the disk coronae, non-stellar optical magnitudes of the active nuclei, or H_β or O III line luminosities), indicate a strong link between the radio production efficiency and the accretion disk parameters, as expected in the case of a jet origin for the radio emission (Ho 2002; Ho & Peng 2001; Panessa et al. 2006, 2007).

The synchrotron/jet origin of the compact cores observed in local low-luminosity AGN is supported by the direct detections of nuclear jets in these systems (Kukula et al. 1999; Middelberg et al. 2004; Ulvestad et al. 1998). Interestingly, observations of the proper motions of such structures indicate sub-relativistic bulk velocities on sub-pc/pc-scales, $v < 0.25c$ (Middelberg et al. 2004; Ulvestad et al. 1999a,b). Note that the observed brightness temperatures of the radio cores in Seyferts and LINERs, as well as their moderate year-timescale variability, do not require relativistic beaming (Mundell et al. 2000). Also, the observed one-sideness of nuclear jets in these systems is best explained as resulting from free-free absorption of radio photons on the surrounding gaseous disks, and not due to relativistic (Doppler) effects (Middelberg et al. 2004). This constitutes a clear difference with the established properties of radio galaxies and quasars.

We also emphasize that the distribution of nuclear jets in Seyferts and LINERs is random with respect to the host galaxy stellar disks (Kinney et al. 2000; Nagar & Wilson 1999; Pringle et al. 1999; Schmitt et al. 2001, 2002; Thean et al. 2001). Moreover, misalignments between sub-pc/pc-scale jets and kpc-scale radio structures are common in Seyferts, being much larger than those observed in other radio-loud AGN (Colbert et al. 1996; Gallimore et al. 2006; Kharb et al. 2006; Middelberg et al. 2004). The appropriate misalignment angle distribution is flat over the whole range 0° to 90° (Middelberg et al. 2004). This may suggest that kpc-scale radio structures are not powered by the jets, but rather originate in starforming regions. Such an interpretation is sometimes supported by the fact that the extended radio-emitting halos in some Seyferts and LINERS are aligned with the galaxy disks, and that their radio powers correlate with the FIR fluxes as observed in regular spiral and starforming galaxies (Thean et al. 2001).

However, in most of the cases ($\geq 45\%$) the observed kpc-scale radio structures of Seyferts and LINERs do not morphologically match those of galaxy disks or starforming regions, showing also excess radio emission over the radio-FIR correlation (Gallimore et al. 2006; Kharb et al. 2006). Thus, such structures are believed to be powered directly by jets, which are, however, substantially different from the ones observed in other radio-loud AGN. In particular, there is growing consensus that Seyferts and LINERs are characterized by

[9] This may however change with the next generation of γ-ray satellites (GLAST) and ground-based Cherenkov Telescopes (like forthcoming next phases of HESS, *Major Atmospheric Gamma-ray Imaging Cherenkov telescope* [MAGIC], or *Very Energetic Radiation Imaging Telescope Array System* [VERITAS]).

short-lived low-power jet activity epochs, with jet lifetimes $t_{\rm j} \lesssim 10^5$ yrs and jet kinetic luminosities $L_{\rm j} \sim 10^{41} - 10^{43}$ erg s^{-1}, possibly triggered by minor accretion episodes, which repeat every $\sim 10^6$ yrs in different (random) directions over the whole Seyfert-type activity epoch $\lesssim$ Gyr (Capetti et al. 1999; Gallimore et al. 2006; Kharb et al. 2006; Sanders 1984).

3. AGN SAMPLE

We collected AGN which are possibly associated with the UHECR events by searching *both* the NASA Extragalactic Database (NED)[10] and the Véron-Cetty & Véron (2006) catalog. Table 1 lists the AGN found within the 3.2° search radius around each UHECR event reported by the Pierre Auger Collaboration (Abraham et al. 2008a), divided into two groups: those within redshift range $z \leq 0.018$ and $0.018 < z \leq 0.037$ (corresponding approximately to the luminosity distances $d_{\rm L} \leq 75$ Mpc and 75 Mpc$\leq d_{\rm L} \leq 150$ Mpc, respectively, Table 2). In total, we have selected 54 active galaxies, 27 per each redshift bin. Note that six UHECR events lack any selected AGN counterpart located within 75 Mpc, and for two of them we also did not find any possible AGN association up to a distance 150 Mpc. Four of these are located at low Galactic latitudes, $|b| < 12^\circ$. Obviously, most of the events possess multiple AGN "counterparts" within the assumed search radius and redshift range.

We emphasize that the Véron-Cetty & Véron (2006) and NED assemblages are not complete AGN catalogs. Additionally, we have found several inconsistencies between these two databases regarding source classifications. This results in a few sources showing some (weak) level of AGN activity (according to one but not the other catalog) which might fulfill the criteria for a possible association with the detected UHECR events, but these are not included in our dataset. However, a few other objects which do not obviously possess an active nucleus (but rather only H II central activity, like NGC 4945, NGC 5244, NGC 2989, NGC 7135, and especially nearby IRAS 13028-49[11]) are included and classified as "possibly LINERs." Furthermore, the regions around 3 events (#7, #12, #16) are covered in the Sloan Digital Sky Survey (SDSS; York et al. 2000) leading to a somewhat misleading higher density of known AGN in these regions in comparison to other event regions. We have therefore omitted the 13 SDSS AGN in the Véron-Cetty & Véron (2006) list falling within the search volume from our Tables. These objects, all classified as Seyferts, are mostly located at redshifts $z > 0.018$ and display similar bulk properties to the Seyferts we have included in our discussion. Most of the selected objects (50 out of 54) are relatively weak Seyfert galaxies and LINERs, while only a small fraction (4) are bright and well established jet sources (three radio galaxies and one BL Lac object). Although few Seyferts/LINERs could be missing/mis-classified in the presented AGN collection, no FR I radio galaxy or BL Lac object is expected to be omitted.

Table 2 lists the main properties of all the selected AGN collected from the literature, in particular the total radio fluxes at 5 GHz (or upper limits for these), *IRAS* fluxes at $60\,\mu$m (if available), and $2 - 10$ keV fluxes (again, if available). In some cases, the flux conversion from values provided at lower radio frequencies (or in higher X-ray photon energy range) was necessary, and we performed this assuming typical values of the radio spectral index $\alpha_R = 0.7$ (X-ray photon index $\Gamma_X = 2.0$). Note that 12 sources listed in Table 2 have only upper limits for the total radio emission (derived by us from the *FIRST*, *NVSS*, or *SUMMS* surveys), and most of them are indeed very weak radio sources (<mJy level).

Only in the case of the four selected FR I/BL Lac sources is the presence of relativistic jets – as ones considered in different models for the acceleration of UHECRs – certain. As for the rest of the selected AGN, one should ask if jet activity can be ascertained and, if so, what are the properties of the jets in these sources. Are these jets relativistic? What are their inclinations? Do they differ somehow from the jets observed in other Seyfert and LINER galaxies? Such questions are relevant, because the space density of the local low-luminosity AGN, just like the ones selected in our sample, is high. For example, the space density of bright galaxies (-22 mag $\leq M_B \leq -18$ mag) showing Seyfert activity is $\sim 1.25 \times 10^{-3}$ Mpc^{-3} (Ulvestad & Ho 2001)[12] which is $\sim 10^2$ times larger than the space density of UHECR sources, $\sim 10^{-5}$ Mpc^{-3}, derived from a comparison of simulation of particle propagation in the local universe and the Akeno Giant Air Shower Array (AGASA) data (Blasi & De Marco 2004; Sigl et al. 2004; Takami et al. 2006). Thus, restricting the investigations to redshifts $z \leq 0.037$, corresponding to the luminosity distance $d_{\rm L} \leq 156.4$ Mpc and comoving volume $V = 0.014$ Gpc^3, there are $\sim 1.8 \times 10^4$ low-luminosity AGN with surface density (if distributed isotropically over the whole sky) $\sim 1.4 \times 10^3$ per steradian. In other words, there should be $\sim$14 AGN within the search radius 3.2°. The much lower rate of our possible identification given in Table 1 is due to incompleteness/lack of the AGN surveys in different parts of the sky, and especially within the Galactic Plane (see a decrease in the identification rate for Galactic latitudes $|b| < 12^\circ$ in Table 1). Thus, if the selected Seyferts and LINERs do not differ from the other local AGN of the same types, the claimed correlation between the UHECR events and local active galaxies should be considered as rather unlikely, resulting from a chance coincidence, if the production of the highest energy CRs is not episodic in nature, but operates in a single object on long ($\geq$ Myr) timescales. In addition, if the selected sources do not show significant jet activity, there are no reasons for expecting them to accelerate CRs up to $10 - 100$ EeV energies at all.

A brief summary of the radio properties of local low-luminosity AGN given in Section 2 allows us to conclude that the particular Seyferts and LINERs selected in Table 2 are most likely jetted, but do not differ from the other analogous sources of the same type. In particular, complex radio morphologies consisting of compact cores, one-sided jets, and extended halos, as found in several of the selected objects, are typical for the Seyfert/LINER-type jet activity. Such jets are expected to be sub-relativistic ($v < 0.25c$ on pc-scales), low-power ($L_{\rm j} \leq 10^{43}$ erg s^{-1}), precessing and short-lived ($t_{\rm j} \lesssim 10^5$ yrs). Indeed, 5 GHz powers for the selected Seyferts and LINERs, being in a range $L_{\rm 5GHz} \sim 10^{37} - 10^{42}$ erg s^{-1}, are typical for the other AGN of the same kind, and are significantly lower than the radio powers of 4 selected radio galaxies/BL Lac. The median values of these, $\sim 2 \times 10^{38}$ erg s^{-1} (including only radio-detected sources), seems to be higher than the appropriate median values given by Ho (2008), but

[10] `http://nedwww.ipac.caltech.edu/`

[11] See Strauss et al. (1992).

[12] This is about $\sim 10^3$ times larger than the local space density of bright quasars, and $\sim$10 times smaller than the space density of "regular" galaxies with comparable brightness (Ulvestad & Ho 2001).

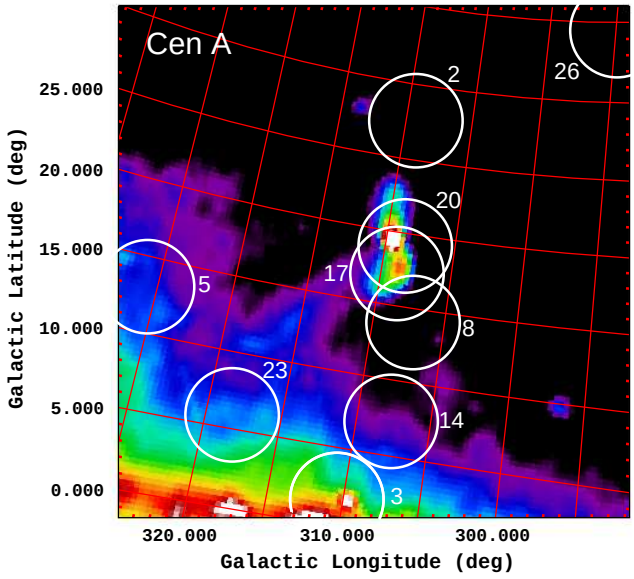

FIG. 1.— Radio map (at 408 MHz from Haslam et al. 1982) of the $35^\circ \times 35^\circ$ field centered on the nearby radio galaxy Centaurus A. The total extent of the north-south radio lobes is $\sim 9^\circ$ and is centered on the AGN (the bright white region near the centre of the field). The $r = 3.2^\circ$ circles mark the positions of the UHECR events detected in the field by Auger (Abraham et al. 2008a). The numbers correspond to the event number as provided in Abraham et al. (2008b), and also in our Table 1. Note event #3 corresponds most closely to Cen B, a bright spot near the center of the circle, shown with higher resolution in Figure 2.

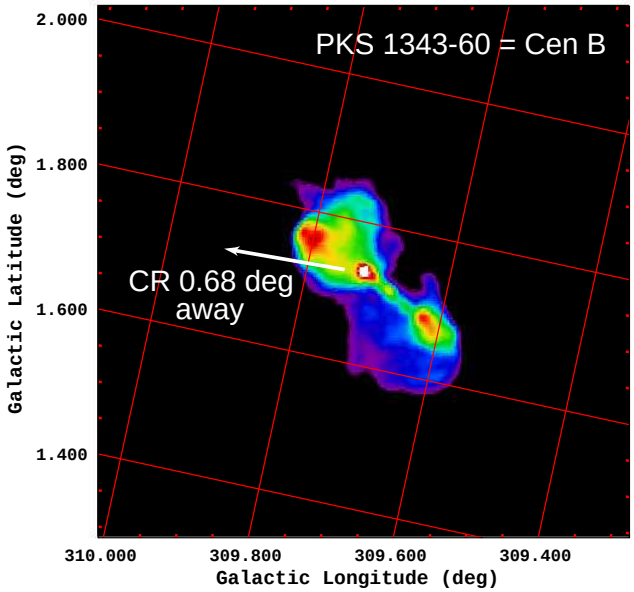

FIG. 2.— Radio image of the $0.75^\circ \times 0.75^\circ$ field centered on the radio galaxy PKS 1343–60 (Cen B). The $43''$ resolution image was obtained with the MOST at 843 MHz by McAdam (1991). The location of the closest CR detected by Auger (#3; c.f. Figure 1) is indicated by the arrow pointing away from the radio nucleus.

this may be simply due to selection effects. In fact, all 12 objects for which only upper limit regarding the radio fluxes are provided, have $L_{5\rm GHz} < 5 \times 10^{37}$ erg s^{-1}.

Also, the X-ray luminosities (if available), being in the range $L_{2-10\rm keV} \sim 10^{40} - 10^{44}$ erg s^{-1} (with the median $\sim 3 \times 10^{41}$ erg s^{-1} again slightly higher than the one provided by Ho 2008), are comparable to the typical $2 - 10$ keV luminosities observed in local low-power AGN (Panessa et al. 2007). Moreover, the logarithm of the ratio of the X-ray and radio luminosities, $\log(L_{5\rm GHz}/L_{2-10\rm keV})$, although widely scattered in a range between (-1.3) and (-5.6) with median (-3.2), is in agreement with the values found in other local low-luminosity AGN (see Panessa et al. 2007).

Finally, the ratio of FIR and radio luminosities for the selected Seyferts and LINERs agrees with what is observed in other analogous sources. Namely, the median value in our sample is $\log(L_{60\mu\rm m}/L_{5\rm GHz}) \sim 5.37$ for Seyferts and LINERs. These can be compared with the medians claimed by Ho & Ulvestad (2001) for Seyferts, ~ 5.31, and for regular spiral galaxies, ~ 5.64, implying that the Seyferts and LINERs included in our sample are not more than twice brighter in radio than expected if all the radio emission is due to star-forming activity, in agreement with the established properties of other Seyferts. We note that the analogous ratios for the two radio galaxies included in the sample and detected at FIR are significantly lower, $\log(L_{60\mu\rm m}/L_{5\rm GHz}) \sim 2.8$ and 3.5, as expected.

3.1. *Selected radio galaxies*

As we already discussed, radio activity in low-power active galaxies of the Seyfert or LINER type differ substantially from that observed in well established jet sources like radio galaxies and radio-loud quasars. Indeed, there are some important reasons for such a difference. In particular, Seyferts and LINERs are usually hosted by spiral (disk) galaxies, while radio galaxies and radio-loud quasars are typically hosted by giant ellipticals. It was noted recently that merger episodes triggering jet activity (by shaping the accretion processes and even determining spins of supermassive black holes[13]), proceed differently depending on the host properties (Hopkins & Hernquist 2006; Sikora et al. 2007; Volonteri et al. 2007).

Of the 54 selected AGN (Table 2), 3 are classified as radio galaxies and one is a BL Lac object, i.e., under the unification scheme, it is a FR I observed with a small jet viewing angle (Urry & Padovani 1995). This group includes NGC 5128 (Cen A; Figure 1), which is characterized by a well-known FR I radio morphology with a one-sided ($\sim$4 kpc long) jet and giant ($\sim$0.5 Mpc) radio lobes (e.g., Israel 1998). This is the only source in the sample detected in γ-rays (Sreekumar et al. 1999; Steinle et al. 1998). Radio maps of PKS 1343–60 (Cen B) reveal a one-sided well-defined FR I jet extending from pc- to kpc-scales, and an edge-brightened structure on the opposite lobe more characteristic of a powerful FR II (Figure 2, Jones et al. 2001). From our new VLA map of PKS 2158–380 (Figure 3), its radio morphology is characteristic of a FR II with bright compact features at the outer edges of its lobes. It is however relatively underluminous for a FR II ($L_{1.4\rm GHz} \sim 4 \times 10^{24}$ W Hz^{-1}) and can be considered an intermediate object. PKS 2201+044 is classified as a BL Lac object with an asymmetric core-jet radio structure (Figure 4), and an extended ($\sim$100 kpc) radio halo (Augusto et al. 1998). These four objects are quite representative of the local population of radio galaxies (note that Cen A is exceptionally bright and extended in the sky only due to its proximity).

Interestingly, due to its large extent on the sky, Cen A may

[13] We note that accordingly to the "spin paradigm", efficiency for the production of relativistic jets in AGN depends on the spin of the supermassive black hole (Blandford 1990).

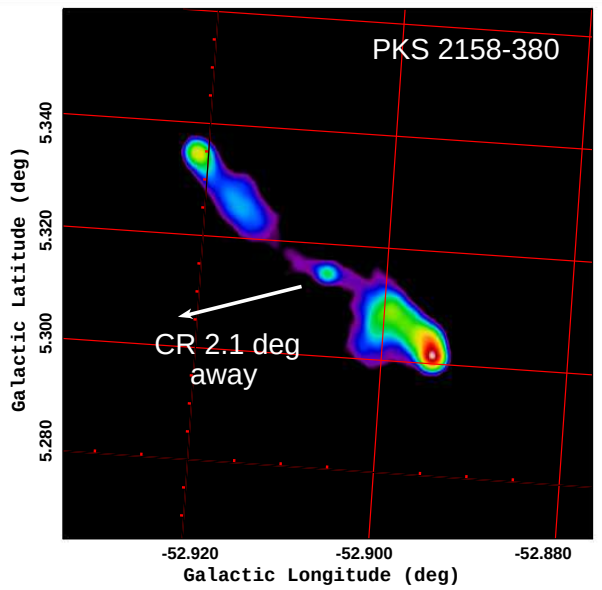

FIG. 3.— Radio image of the $200'' \times 200''$ field around the radio galaxy PKS 2158–380. We obtained the calibrated VLA 4.9 GHz data from the NRAO VLA Archive Survey (NVAS) and performed additional self-calibration and final CLEAN to produce the $5''$ resolution image. The location of the closest cosmic ray detected by Auger (#9) is indicated by the arrow pointing away from the radio nucleus.

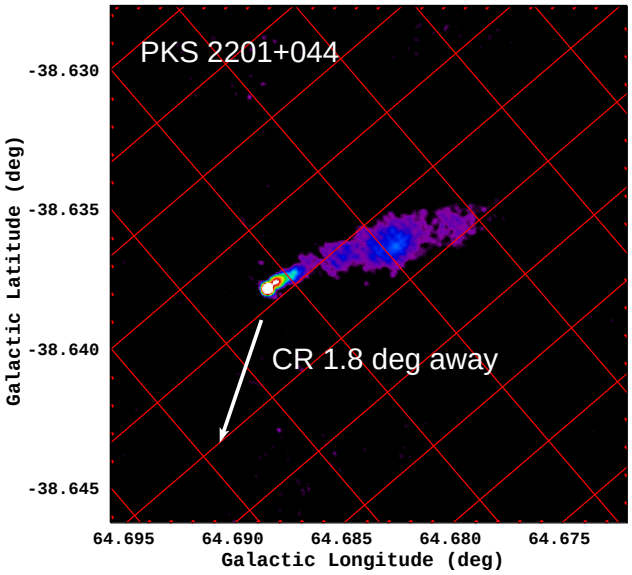

FIG. 4.— Radio image of the $100'' \times 100''$ field around the BL Lac object PKS 2201+044 showing its one-sided radio jet. The image is a lower resolution ($1''$ beam) version of the VLA 8.5 GHz data published in Sambruna et al. (2007). The location of the closest CR detected by Auger (#19) is indicated by the arrow pointing away from the radio nucleus.

be considered as being likely associated with more than two Auger events (see Figure 1). Note that Table 1 indicates a possible association of Cen A with only two CR events, because the 3.2° separation of the UHECR event from the Cen A *nucleus* is assumed when compiling the list of the selected AGN). Considering the 9 events plotted in Figure 1 around the giant radio structure of Cen A, we note that their detection rate appears steady (almost every third event detected by Auger, except for the larger gap between events #8 and #14). If the rate is indeed steady, as would be expected if giant Mpc-scale radio lobes of Cen A are the acceleration sites of these events, this will be easily tested with an additional 2-4 years of Auger observations.

Considering the four events closest to Cen A, the positions of these four events are roughly aligned with the axis of the radio lobes, which is also aligned with the super-galactic plane (cf. Figure 2 of Abraham et al. 2008a). The latter two events are closest to the center of Cen A and the former two are coincident with other AGN in the field. It is of interest to note that one of the field AGN is NGC 4945 (event #8), which is located in the Centaurus group (i.e., it is at the same approximate distance as Cen A). NGC 4945 hosts a less powerful radio source than Cen A and is dominated by extended emission from the galaxy and a compact non-thermal core (Elmouttie et al. 1997). Also, of the 6 UHECR events without an associated nearby ($z < 0.018$) AGN within a $r = 3.2^\circ$ circular area, 2 are in the plotted field (#14, #26). However, #14 is the one closest to the Galactic Plane, where it is more difficult to identify AGN, and #26 is the one furthest from Cen A. As discussed in the next Section a larger deflection angle for the events close to the Galactic plane is possible, which could mean that Cen B could be associated with more than 1 event.

4. PROPAGATION AND COMPOSITION OF UHECRS

The propagation of the UHECRs from the sources to the observer is not rectilinear due to deflection by intervening magnetic fields. The magnetic field structure (both extragalactic and Galactic), along with the UHECR source distribution, the nature of sources (transient vs. steady), the energy spectrum at the injection, and the CR composition, are all factors that affect the distribution of the observed arrival directions.

Though quite an extensive literature on simulation of UHECR propagation in the extragalactic magnetic field exists, very little is known about the strength and configuration of such fields. So far, direct evidence for the presence of extragalactic magnetic fields has been found only in galaxy clusters (for a review see Carilli & Taylor 2002). Faraday rotation measurements provide evidence for intracluster core fields in the range of $1 - 10$ μG. Outside clusters only upper limits at the level $1-10$ nG are available. Extragalactic magnetic fields are *ad hoc* assumed to have a domain structure with a Kolmogorov power spectrum and a uniform correlation length. Toy models assume a field strength $\sim$1 nG in voids with a somewhat larger field $\sim$10 nG at the supergalactic plane (e.g., Stanev et al. 2003).

Recent simulations of magnetic fields in the intergalactic medium are more sophisticated. They take into account the growth of the magnetic fields from seed fields such that the resulting field strength traces the baryon density as the large-scale structure evolves. A more realistic extragalactic magnetic field of this nature may result in significantly larger deflections than is expected from a purely random field. A simulation by Sigl et al. (2004) used the Biermann battery mechanism to generate seed fields which were evolved, and then rescaled so that the magnetic field in the core of a simulated Coma-like galaxy cluster is comparable to the μG fields as indicated by Faraday rotation measures. Simulations of large-scale structure formation and the build-up of magnetic fields in the intergalactic medium have also been performed by Dolag et al. (2005). The basic assumption is that cosmological magnetic fields grow in a magnetohydrodynamic amplification process driven by the formation of structure from a

magnetic seed field present at high redshift. The initial density fluctuations were constructed from the IRAS 1.2-Jy galaxy survey by first smoothing the observed galaxy density field on a scale of 7 Mpc, evolving it linearly back in time and then using it as a Gaussian constraint for an otherwise random realization of a ΛCDM cosmology (Mathis et al. 2002). As a result, the positions and masses of prominent galaxy clusters coincide closely with their real counterparts in the local universe. Takami et al. (2006) have used a magnetic field strength scaled with the matter density $|B| \propto \rho^{2/3}$, where the distribution of galaxies is constructed using the IRAS PSCz catalog. The correlation length is taken to be 1 Mpc and the magnetic field is assumed to be represented as a Gaussian random field with a Kolmogorov power spectrum in each cube. The field is further renormalized to obtain ∼0.4 μG in a cube that contains the center of the Virgo Cluster.

The deflection angle in a random field is $\theta_d \approx 2.5^\circ Z E_{20}^{-1} B_{-9} (D_{100} l_1)^{1/2}$, where Z is the particle charge, D_{100} is the distance in units 100 Mpc, B_{-9} is the r.m.s. field strength in nG, E_{20} is the particle energy in units 10^{20} eV, and l_1 is the correlation length in Mpc (e.g., Sigl et al. 2004). The time delay corresponding to θ_d can be estimated as $\tau \sim 1.5 \times 10^5 Z^2 E_{20}^{-2} B_{-9}^2 D_{100}^2 l_1$ yr. For a 10^{20} eV proton injected at $D \sim 75$ Mpc for characteristic values of $B_{-9} \sim 1$ and $l_1 \sim 1$, $\theta_d \sim 2^\circ$ and $\tau \sim 1.2 \times 10^5$ yr which is comparable to the crossing time of the Galaxy and the characteristic timescale of jet lifetimes in Seyfert galaxies as discussed earlier, but is negligible compared to the galactic evolution timescale. Therefore, observations at different wavelengths show us *nearly* a snapshot of the sources at the time when the highest energy CRs were emitted. If a detected CR particle has been accelerated by a pc-scale jet, the jet will expand during the time delay to become larger, $\gtrsim 10^5$ lt-yr, and this may be seen as a more extended structure in the radio. The association of UHECR accelerators must correspondingly take into account such time delays and source evolution since observed photon signals come from later times than the epoch of UHECR escape from the source.

The Galactic magnetic field is known much better than the extragalactic one. It can be determined from pulsar rotation and dispersion measures combined with a model for the distribution of free electrons (e.g., Cordes & Lazio 2003a,b). A large-scale field of a few μG aligned with the spiral arms exists, but there is no general agreement on the details (Beck 2001). Recent studies give a bisymmetric model for the large-scale Galactic magnetic field with reversals on arm-interarm boundaries (Brown et al. 2007; Han 2008; Han et al. 2006). Independent estimates of the strength and distribution of the field can be made by simultaneous analysis of radio synchrotron, CR, and γ-ray data, and these confirm a value of a few μG, increasing towards the inner Galaxy (Strong et al. 2000, and Strong et al. *in prep.*). The magnetic field in the halo is less known. Observations of the rotation measure of extragalactic radio sources reveal azimuth magnetic fields in the halo with reversed directions below and above the plane consistent with A0 symmetry type (Han 2008; Wielebinski & Krause 1993).

Because of their large Larmor radii >1 kpc ($r_L \approx 10^5 E_{20}/B_{-9}$ kpc), UHECRs propagating in the Galactic magnetic field are sensitive to the global topology of the field. The influence of the geometry of the Galactic magnetic field has been studied in various source distribution scenarios (Alvarez-Muñiz 2002; Stanev 1997; Takami et al. 2006). For a ∼1 μG magnetic field, the distance $D \sim 100$ kpc, and a correlation length $l \sim 1$ kpc, the average deflection angle is $\theta_d \sim 2.5^\circ E_{20}^{-1}$, but the actual value depends on the arrival direction of a CR particle. It is interesting to note that Cen A is only ∼50° away in longitude from the Galactic Centre, and only ∼20° from the Galactic plane, while Cen B is very close ∼1° to the Galactic equator. Cosmic rays coming from either of these objects could be influenced by the stronger magnetic field near the Galactic plane (a few μG vs. ∼1 μG in the Galactic halo) over tens of kpcs of their trajectory. This would provide a greater deflection than the relatively longer pathlength through the weak extragalactic magnetic field. Therefore, an association of Cen A and Cen B with more events in this region could be possible.

The UHECR source distribution is usually assumed homogeneous or to follow the baryon density distribution. The former case is relevant for energies below the photopion production threshold for proton injection where the energy losses are small and particles may come from cosmological distances. Since only a small fraction of the sky is covered with the extragalactic magnetic field capable of deflecting UHECR particles by a significant angle (Dolag et al. 2005), the resulting distribution of arrival directions is close to isotropic (Takami et al. 2006). If the energy of CRs is near the GZK cutoff, the sources are likely local. In this case the distribution of sources traces the baryon density distribution in the local Universe and the effective field acting on UHECRs is considerably stronger, leading to larger deflection angles which can be as large as ∼20° at 10^{20} eV (Sigl et al. 2004). In this case, the arival directions of UHECRs (Abraham et al. 2007b) should correlate with the distribution of large deflections on a deflection map; such a correlation can be seen even from a by-eye comparison with the deflection map given by Takami et al. (2006, their Figure 5). Such sources should also be capable of producing lower energy CRs and γ-rays (and neutrinos) and, therefore, may be observed with the next generation γ-ray telescopes.

Most of our discussion has described the situation if the UHECRs particles are protons. This is complicated further if the injected particles are CR nuclei since the deflection angles can be larger for a given magnetic field and the nuclei undergo photodisintegration processes on the CMB and extragalactic infrared background fragmenting into lighter nuclei (e.g., Stecker & Salamon 1999). The UHECR chemical composition is unknown and subject to considerable debate. Results from the surface arrays AGASA (Shinozaki 2006) and Yakutsk (Knurenko et al. 2008) and fluorescence detectors (e.g., Sokolsky & Thomson 2007, and references therein) indicate a trend toward proton dominated composition at the highest energies. However, the Pierre Auger Collaboration has presented a fit to the elongation rate[14] (Unger et al. 2007) showing a heavier or mixed composition at the highest energies. These interpretations are complicated by the necessary reliance on hadronic interaction models which have to extrapolate cross section information beyond current accelerator energies, and indeed even details of the UHECR sources themselves can introduce degeneracy in the interpretation of the data with different chemical compositions (e.g., Arisaka et al. 2007). It has been argued recently (e.g., Dermer 2008; Fargion 2008; Hooper et al. 2008) that the current anisotropy results can be explained if the composition has

[14] The elongation rate is the slope $dX_{\max}/d\log E$, where $X_{\max}$ is the depth of shower maximum.

a significant component of light nuclei, $4 \leq A \leq 14$, but this remains to be tested by further data.

5. CONCLUSION

A transition from an isotropic distribution of arrival directions of CRs above $\sim$1 EeV (Watson 2008) to an anisotropic distribution of the highest-energy CRs above 57 EeV (Abraham et al. 2007a) observed by the Pierre Auger Collaboration implies a change in the propagation mode of UHECRs in intergalactic and/or Galactic space. The association of the observed events with the supergalactic plane points to the sources tracing the supergalactic plane and matter distribution which correlates with AGN. However, as we have shown, almost all nearby ($d_{\rm L} \leq 150\,$Mpc) active galaxies found within the search radii of 3.2° around the UHECR events detected by the Pierre Auger Collaboration are typical for the local low-luminosity AGN of the Seyfert/LINER type. They are characterized by low-power and short jet activity, which is substantially different from that observed in radio galaxies and quasars (as typically considered in the scenarios for acceleration of UHECRs). Moreover, such selected low-luminosity AGN are expected to be quite common in the local Universe, with the estimated surface density 1.4×10^3 per steradian, when limited to a redshift $z \leq 0.037$. Hence, we conclude that the correlation with particular AGN is a coincidence. A future, more extensive analysis has to take into account details of the AGN radio morphology and spectral properties, and may yield a correlation with a larger deflection angle and/or more distant sources.

We emphasize that there is no complete all-sky catalog of nearby AGN. In addition, many "regular" galaxies when studied at sufficient spatial resolution at different wavelengths show some (typically weak) level of the AGN-like activity. Hence, the confusion in classification of such sources in the literature, different databases, and catalogs. Thus, investigating the correlation of UHECRs with AGN based on some given particular AGN catalog may be tricky and even meaningless. In particular, using catalogs of X-ray selected local active galaxies may give misleading results since the X-ray emission of Seyferts and LINERs is produced by the accretion disks and the disk coronae, and therefore represents the accretion power of the active nucleus rather than the power of its jet. Although the most recent studies have found a correlation between the disk luminosity and the radio power of the unresolved nucleus (Ho 2002; Ho & Peng 2001; Panessa et al. 2006, 2007), the former has no direct relation with the large-scale radio structures which are supposed to be capable of accelerating CRs up to the highest energies. Instead, as argued in this paper, the spectral and morphological properties of the *jetted* AGN which are selected as likely counterparts of the detected UHECR events should be considered in detail and compared with the properties of the parent population: are the selected sources in some respect substantially different from all other nearby and numerous low-luminosity active galaxies? Although few Seyferts/LINERs could be missing/misclassified in the presented AGN collection, no FR I radio galaxy or BL Lac object is expected to be omitted.

Other possibilities include a few close sources with extended jet/lobe structures, such as Cen A and Cen B, and relatively large deflections due to either strong magnetic fields or due to the presence of heavy nuclei in the flux, or more distant sources.

Observations with γ-ray telescopes, such as GLAST, HESS, MAGIC, and VERITAS may point to the *class of sources* able to accelerate particles to TeV energies, and are therefore potentially capable of accelerating particles up to EeV energies. Such sources could also produce TeV and UHE neutrinos. Taking into account the delay between the arrival times of γ-rays (neutrinos) and UHECRs, such observations have to be interpreted with care: UHECRs may come from sources which are not generating TeV γ-rays anymore, or UHECRs that are accelerated in present day γ-ray emitters have not had time to propagate to us, yet. Meanwhile, Cen A and Cen B are two powerful sources cosmologically nearby and, if they are indeed UHECR sources, γ-ray observations can provide a "current" picture at the time when the CRs were emitted since the overall time delay from propagation is very short. Moreover, Cen A is large enough to be resolved by γ-ray instruments (e.g., McEnery et al. 2004). Therefore, observations with γ-ray telescopes may provide additional clues to the origin of UHECRs.

I. V. M. acknowledges support from NASA Astronomy and Physics Research and Analysis Program (APRA) grant. Ł. S. acknowledge support by the MEiN grant 1-P03D-003-29. T. A. P. acknowledges partial support from the US Department of Energy. C.C.C. was supported by an appointment to the NASA Postdoctoral Program at Goddard Space Flight Center, administered by Oak Ridge Associated Universities through a contract with NASA. This research has made use of the NASA/IPAC Extragalactic Database (NED) which is operated by the Jet Propulsion Laboratory, California Institute of Technology, under contract with NASA.

REFERENCES

Abbasi, R. U., et al. 2005, ApJ, 622, 910
Abraham, J., et al. 2007, APh, 27, 155
Abraham, J., et al. 2007, Science, 318, 938
Abraham, J., et al. 2008, APh, 28, 188
Abraham, J., et al. 2008, APh, 29, 243
Alvarez-Muñiz, J., Engel, R., & Stanev, T. 2002, ApJ, 572, 185
Antonucci, R. 1993, ARA&A, 31, 473
Arisaka, K., et al. 2007, JCAP, 12, 2
Augusto, P., Wilkinson, P. N., & Browne, I. W. A. 1998, MNRAS, 299, 1159
Baum, S. A., et al. 1993, ApJ, 419, 553
Beck, R. 2001, Space Sci. Rev., 99, 243
Becker, R. H., White, R. L., & Helfand, D. J. 1995, ApJ, 450, 559
Beckmann, V., Gehrels, N., Shrader, C. R., & Soldi, S. 2006, ApJ, 638, 642
Begelman, M. C., Blandford, R. D., & Rees, M. J. 1984, Rev. Mod. Phys., 56, 255
Berezinsky, V., Gazizov, A., & Grigorieva, S. 2006, Phys. Rev. D, 74, 043005
Biermann, P. L., & Strittmatter, P. A. 1987, ApJ, 322, 643
Bird, A. J., et al. 2007, ApJS, 170, 175
Blandford, R.D., 1990, in Active Galactice Nuclei, ed. T.J.-L. Courvoisier & M. Mayor (Saas-Fee Advanced Course 20, Berlin:Springer), 161
Blasi, P., & De Marco, D. 2004, APh, 20, 559
Bock, D. C.-J., Large, M. I., & Sadler, E. M. 1999, AJ, 117, 1578
Brinkmann, W., Siebert, J., & Boller, Th. 1994, A&A, 281, 355
Brown, J. C., et al. 2007, ApJ, 663, 258
Capetti, A., et al. 1999, ApJ, 516, 187
Carilli, C. L., & Taylor, G. B. 2002, ARA&A, 40, 319
Celotti, A., & Ghisellini, G. 2008, MNRAS, 385, 283
Colbert, E. J. M., et al. 1996, ApJ, 467, 551
Condon, J. J., Helou, G., Sanders, D. B., & Soifer, B. T. 1990, ApJS, 73, 359
Condon, J. J., et al. 1998, AJ, 115, 1693
Condon, J. J., Cotton, W. D., & Broderick, J. J. 2002, AJ, 124, 675
Cordes, J. M., & Lazio, T. J. W. 2003a, preprint (arXiv: astro-ph/0207156)
Cordes, J. M., & Lazio, T. J. W. 2003b, preprint (arXiv: astro-ph/0301598)
Dermer, C. D. 2007, preprint (arXiv: 0711.2804)
Dermer, C. D. 2008, preprint (arXiv: 0804.2466)
Dolag, K., Grasso, D., Springel, V., & Tkachev, I. 2005, JCAP, 01, 009

Elmouttie, M., et al. 1997, MNRAS, 284, 830
Fanaroff, B. L., & Riley, J. M. 1974, MNRAS, 167, 31
Fargion, D. 2008, preprint (arXiv: 0801.0227)
Gallimore, J. F., Baum, S. A., & O'Dea, C. P. 1997, Nature, 388, 852
Gallimore, J. F., et al. 2006, AJ, 132, 546
Gonzalez-Martin, O., et al. 2006, A&A, 460, 45
Gorbunov, D. S., Tinyakov, P. G., Tkachev, I. I., & Troitsky, S. V. 2008, preprint (arXiv: 0804.1088)
Gregory, P. C., Vavasour, J. D., Scott, W. K., & Condon, J. J. 1994, ApJS, 90, 173
Greisen, K. 1966, Phys. Rev. Lett., 16, 748
Guainazzi, M., Matt, G., & Perola, G. C. 2005, A&A, 444, 119
Han, J. L. 2008, Nucl. Phys. B (Proc. Suppl.), 175, 62
Han, J. L., et al. 2006, ApJ, 642, 868
Haslam, C. G. T., Salter, C. J., Stoffel, H., & Wilson, W. E. 1982, A&AS, 47, 1
Hillas, A. M. 1984, ARA&A, 22, 425
Helou, G., Soifer, B. T., & Rowan-Robinson, M. 1985, ApJ, 298, 7
Ho, L. C. 2002, ApJ, 564, 120
Ho, L. C. 2008, ARA&A, in press (arXiv: 0803.2268)
Ho, L. C., & Peng, C. Y. 2001, ApJ, 555, 650
Ho, L. C., & Ulvestad, J. S. 2001, ApJS, 133, 77
Hooper, D., et al. 2008, preprint (arXiv: 0802.1538)
Hopkins, P. F., & Hernquist, L. 2006, ApJS, 166, 1
Israel, F. P. 1998, Astron. Astrophys. Rev., 8, 237
Jones, P. A., & McAdam, W. B. 1992, ApJS, 80, 137
Jones, P. A., Lloyd, B. D., & McAdam, W. B. 2001, MNRAS, 325, 817
Karachentsev, I. D., et al. 2007, AJ, 133, 504
Kharb, P., et al. 2006, ApJ, 652, 177
Kinney, A. L., et al. 2000, ApJ, 537, 152
Knurenko, S. P., et al. 2008, Nucl. Phys. B (Proc. Suppl.), 175, 201
Kukula, M. J., Ghosh, T., Pedlar, A., & Schilizzi, R. T. 1999, ApJ, 518, 117
Lutz, D., Maiolino, R., Spoon, H. W. W., & Moorwood, A. F. M. 2004, A&A, 418, 465
Lyutikov, M., & Ouyed, R. 2007, APh, 27, 473
Marshall, H. L., et al. 2005, ApJS, 156, 13
Mathis, H., et al. 2002, MNRAS, 333, 739
Mauch, T., et al. 2003, MNRAS, 342, 1117
McAdam, W. B. 1991, Proceedings of the Astronomical Society of Australia, 9, 255
McEnery, J. E., Moskalenko, I. V., & Ormes, J. F., 2004, in Cosmic Gamma-Ray Sources, eds. K. Cheng & G. E. Romero, (Dordrecht: Kluwer), Astrophys. & Spa. Sci. Library, v.304, 361 (arXiv: astro-ph/0406250)
Middelberg, E., et al. 2004, A&A, 417, 925
Mollenhoff, C., Hummel, E., & Bender, R. 1992, A&A, 255, 35
Morganti, R., Tsvetanov, Z. I., Gallimore, J., & Allen, M. G. 1999, A&AS, 137, 457
Moshir, M., et al. 1990, IRAS Faint Source Catalogue, version 2.0
Mundell, C. G., Wilson, A. S., Ulvestad, J. S., & Roy, A. L. 2000, ApJ, 529, 816
Nagano, M., & Watson, A. A. 2000, Rev. Mod. Phys., 72, 689
Nagar, N. M., & Wilson, A. S. 1999, ApJ, 516, 97
Nagar, N. M., Wilson, A. S., Mulchaey, J. S., & Gallimore, J. F. 1999, ApJS, 120, 209
Nagar, N. M., Falcke, H., & Wilson, A. S. 2005, A&A, 435, 521
Ostrowski, M. 1998, A&A, 335, 134
Ostrowski, M. 2002, APh, 18, 229
Panessa, F., et al. 2006, A&A, 455, 173
Panessa, F., et al. 2007, A&A, 467, 519
Pringle, J. E., et al. 1999, ApJ, 526, 9
Roy, A. L., et al. 1998, MNRAS, 301, 1019
Rush, B., Malkan, M. A., & Edelson, R. A. 1996, ApJ, 473, 130
Sadler, E. M., Jenkins, C. R., & Kotanyi, C. G. 1989, MNRAS, 240, 591
Sambruna, R. M., et al. 2007, ApJ, 670, 74
Sanders, R. H. 1984, A&A, 140, 52
Schmitt, H. R., et al. 2001, ApJ, 555, 663
Schmitt, H. R., Pringle, J. E., Clarke, C. J., & Kinney, A. L. 2002, ApJ, 575, 150
Shinozaki, K., et al. 2006, AJ, 131, 2843
Shinozaki, K. [AGASA Collaboration] 2006, Nucl. Phys. B (Proc. Suppl.), 151, 3
Sigl, G., Miniati, F., & Ensslin, T. A. 2004, Phys. Rev. D, 70, 043007
Sikora, M., Stawarz, Ł., & Lasota, J.-P. 2007, ApJ, 658, 815
Sokolsky, P., & Thomson, G. B. 2007, J. Phys. G: Nucl. Part. Phys., 34, R401
Sreekumar, P., et al. 1999, APh, 11, 221
Stanev, T. 1997, ApJ, 479, 290
Stanev, T. 2007, Proc. 30th Int. Cosmic Ray Conf. (Merida), in press; arXiv:0711.2282
Stanev, T. 2007, Nucl. Phys. B (Proc. Suppl.), 168, 252
Stanev, T., Seckel, D., & Engel, R. 2003, Phys. Rev. D, 68, 103004
Stecker, F. W. & Salamon, M. H. 1999, ApJ, 512, 521
Steinle, H., et al. 1998, A&A, 330, 97
Strauss, M. A., et al. 1992, ApJS, 83, 29
Strong, A. W., Moskalenko, I. V., & Reimer, O. 2000, ApJ, 537, 763
Svensson, R. 1996, A&AS, 120, 475
Tajer, M. et al. 2005, A&A, 435, 799
Takami, H., Yoshiguchi, H., & Sato, K. 2006, ApJ, 639, 803
Thean, A., et al. 2001, MNRAS, 325, 737
Ueda, Y., et al. 2005, ApJS, 161, 185
Ulvestad, J. S., & Wilson, A. S. 1989, ApJ, 343, 659
Ulvestad, J. S., & Ho, L. C. 2001, ApJ, 558, 561
Ulvestad, J. S., Roy, A. L., Colbert, E. J. M., & Wilson, A. S. 1998, ApJ, 496, 196
Ulvestad, J. S., Wrobel, J. M., & Carilli, C. L. 1999a, ApJ, 516, 127
Ulvestad, J. S., et al. 1999b, ApJ, 517, L81
Unger, M., et al. [Pierre Auger Collaboration] 2007, Proc. 30th Int. Cosmic Ray Conf. (Merida), in press
Urry, C. M. & Padovani, P. 1995, PASP, 107, 803
Véron-Cetty, M.-P., & Véron, P. 2006, A&A, 455, 773
Volonteri, M., Sikora, M., & Lasota, J.-P. 2007, ApJ, 667, 704
Watson, A. A. 2008, Nucl. Instr. Meth. Phys. Res. A, 588, 221
White, R. L., & Becker, R. H. 1992, ApJS, 79, 331
Wielebinski, R., & Krause, F. 1993, Astron. Astrophys. Rev., 4, 449
Wright, A., & Otrupcek, R. 1990, Parkes Catalog (PKS Catalog: Australia telescope national facility)
York, D. G., et al. 2000, AJ, 120, 1579
Zatsepin, G. T., & Kuz'min, V. A. 1966, JETP Lett., 4, 78
Zdziarski, A. A., 1999, in High Energy Processes in Accreting Black Holes, eds. J. Poutanen & R. Svensson, ASP Conference Series 161, 16

TABLE 1. AGN POSSIBLY ASSOCIATED WITH UHECRS EVENTS

UHECR Event		AGN within 3.2° search radius			
Event number	Galactic Coordinates	$0 < z \leq 0.018$		$0.018 < z \leq 0.037$	
	(ℓ [°], b [°])	Name	θ [′]	Name	θ [′]
25	(−21.8, 54.1)	NGC 5506	38	UM 653	136
				UM 654	138
				UM 625	171
18	(−57.2, 41.8)			ESO 575-IG016	55
				MCG-03-32-017	191
26	(−65.1, 34.5)			TOLOLO 00020	133
2	(−50.8, 27.6)	NGC 5140	116	2MASX J13230241-3452464	55
				TOLOLO 00081	95
				ESO 444-G018	144
21	(−109.4, 23.8)	NGC 2907	94		
		NGC 2989	182		
20	(−51.4, 19.2)	NGC 5128⋆	54		
17	(−51.2, 17.2)	NGC 5128⋆	139		
		NGC 5064⋆	162		
		NGC 5244	164		
8	(−52.8, 14.1)	NGC 5064⋆	47		
		IRAS 13028-4909	118		
		NGC 4945	121		
5	(−34.4, 13.0)	IC 4518A	66		
1	(15.4, 8.4)			1RXS J174155.3-121157	106
				HB91 1739-126	122
14	(−52.3, 7.3)			WKK 2031	83
23	(−41.7, 5.9)	WKK 4374	167		
3	(−49.6, 1.7)	DZOA 4653-11	40		
		PKS 1343-60	41		
27	(−125.2, −7.7)				
11	(−103.7, −10.3)				
13	(−27.6, −16.5)	ESO 139-G012⋆	109		
		AM 1754-634 NED03⋆	191		
4	(−27.7, −17.0)	ESO 139-G012⋆	139		
		AM 1754-634 NED03⋆	166		
10	(48.8, −28.7)	CGCG 374-029	183	PC 2055+0126	125
				Mrk 510	152
19	(63.5, −40.2)	PC 2207+0122⋆	98	PKS 2201+044	109
				NGC 7189⋆	151
7	(58.8, −42.4)	PC 2207+0122⋆	189	NGC 7189⋆	108
16	(−170.6, −45.7)	NGC 1358⋆	51	Mrk 612	81
		NGC 1320	130	Mrk 609⋆	133
				KUG 0322-063A⋆	137
12	(−165.9, −46.9)	NGC 1346	152	Mrk 609⋆	169
		NGC 1358⋆	166	KUG 0322-063A⋆	171
15	(88.8, −47.1)	NGC 7626	86	2MASX J23274259+0845298	122
		NGC 7591	186	NGC 7674	125
24	(12.1, −49.0)	NGC 7130	117	6dF J2132022-334254	127
		NGC 7135	126		
22	(−163.8, −54.4)	NGC 1204	96	MCG-02-08-039	174
9	(4.2, −54.9)	IC 5169	131	ESO 404-IG042	76
				PKS 2158-380	126
6	(−75.6, −78.6)	NGC 0424	25	ESO 351-G025	153
				ESO 352-G048	163

NOTE. — θ denotes the separation between an UHECR event and an AGN. Stars denote AGN falling within the 3.2° search radius of two different events.

TABLE 2. PROPERTIES OF SELECTED AGN

Name	Type	RA (J2000.0)	DEC (J2000.0)	z	$d_{\rm L}$ [Mpc]	UHECR ($\ell\,[^\circ]$, $b\,[^\circ]$)	θ [$'$]	$S_{\rm R}$ [mJy]	Ref.	$S_{\rm FIR}$ [Jy]	$S_{\rm X}$ [cgs]	Ref.
(1)	(2)	(3)	(4)	(5)	(6)	(7)	(8)	(9)	(10)	(11)	(12)	(13)
NGC 5506	Sy2	14h13m14.8s	−03d12m27s	0.0062	29	(−21.8, 54.1)	38	227	G06	8.4	12	S06
UM 653	Sy2	14h16m15.5s	−01d27m53s	0.0365	158	(−21.8, 54.1)	136	0.9^c	B95	0.4	—	—
UM 654	Sy2	14h16m19.7s	−01d25m18s	0.0369	160	(−21.8, 54.1)	138	$<0.2^c$	B95	—	—	—
UM 625	Sy2	14h00m40.6s	−01d55m18s	0.0250	109	(−21.8, 54.1)	171	1.1^c	B95	0.3	—	—
ESO 575-IG016	S2	12h52m36.2s	−21d54m46s	0.0229	100	(−57.2, 41.8)	55	1.7^c	C98	—	—	—
MCG-03-32-017	L(?)	12h38m00.5s	−20d07m51s	0.0280	123	(−57.2, 41.8)	191	$<0.8^c$	C98	—	—	—
TOLOLO 20	Sy1	12h12m20.0s	−28d48m46s	0.0300	131	(−65.1, 34.5)	133	$<0.5^c$	C98	—	—	—
2MASX J1323	L(?)	13h23m02.4s	−34d52m47s	0.0261	113	(−50.8, 27.6)	55	10.8^c	C98	—	—	—
TOLOLO 81	Sy2	13h19m38.6s	−33d22m54s	0.0291	127	(−50.8, 27.6)	95	$<0.8^c$	C98	—	—	—
NGC 5140	L(?)	13h26m21.7s	−33d52m06s	0.0129	58	(−50.8, 27.6)	116	29.2	S89	0.8	—	—
ESO 444-G018	L(?)	13h22m56.8s	−32d43m42s	0.0292	127	(−50.8, 27.6)	144	7.5^c	C98	—	—	—
NGC 2907	L(?)	09h31m36.7s	−16d44m05s	0.0070	33	(−109.4, 23.8)	94	4.4^c	M92	0.4	—	—
NGC 2989	L(?)	09h45m25.2s	−18d22m26s	0.0138	62	(−109.4, 23.8)	182	7.6^c	C98	1.7	—	—
NGC 5128	FR I	13h25m27.6s	−43d01m09s	0.0018	3.4	(−51.4, 19.2)	54	53792	G94	162	30	B06
						(−51.2, 17.2)	139					
NGC 5064	L	13h18m59.9s	−47d54m31s	0.0099	45	(−51.2, 17.2)	162	4.0^c	M03	3.3	—	—
						(−52.8, 14.1)	47					
NGC 5244	L(?)	13h38m41.7s	−45d51m21s	0.0085	38	(−51.2, 17.2)	164	5.7^c	M03	1.9	—	—
IRAS 13028-49	Sy(?)	13h05m45.5s	−49d25m22s	0.0012	8.3	(−52.8, 14.1)	118	$<22^c$	B99	6.1	—	—
NGC 4945	Sy(?)	13h05m27.5s	−49d28m06s	0.0019	3.8	(−52.8, 14.1)	121	2953	G94	359	0.5	L04
IC 4518A	S2	14h57m41.2s	−43d07m56s	0.0163	70	(−34.4, 13.0)	66	64.9^c	M03	—	1.9^h	B07
1RXS J174155	Sy1	17h41m55.3s	−12d11m57s	0.0370	156	(15.4, 8.4)	106	1.4^c	C98	—	2.9^h	B07
HB91 1739-126	Sy1	17h41m48.7s	−12d41m01s	0.0370	156	(15.4, 8.4)	122	$<0.5^c$	C98	—	—	—
WKK 2031	S2	13h15m06.3s	−55d09m23s	0.0308	133	(−52.3, 7.3)	83	154	G94	41.0	—	—
WKK 4374	Sy2	14h51m33.1s	−55d40m38s	0.0180	77	(−41.7, 5.9)	167	6.2^c	B99	—	2.0^h	B07
DZOA 4653-11	Sy1	13h47m36.0s	−60d37m04s	0.0129	56	(−49.6, 1.7)	40	$<3.8^c$	B99	—	7.8^h	B07
PKS 1343-60	FR I	13h46m49.0s	−60d24m29s	0.0129	56	(−49.6, 1.7)	41	27100	W90	—	0.2^l	M05
ESO 139-G012	Sy2	17h37m39.1s	−59d56m27s	0.0170	71	(−27.6, −16.6)	109	5.2^c	M03	0.7	—	—
						(−27.7, −17.0)	139					
AM 1754-634	Sy(?)	18h00m10.9s	−63d43m34s	0.0157	65	(−27.6, −16.5)	191	$<0.9^c$	B99	—	—	—
						(−27.7, −17.0)	166					
PC 2055+0126	S(?)	20h58m18.2s	+01d38m00s	0.0260	105	(48.8, −28.7)	125	$<0.8^c$	C98	—	—	—
Mrk 510	Sy(?)	21h09m23.0s	−01d50m17s	0.0195	77	(48.8, −28.7)	152	48.4^c	W92	—	—	—
CGCG 374-029	S1	20h55m22.3s	+02d21m16s	0.0136	52	(48.8, −28.7)	183	1.8^c	C98	—	—	—
PC 2207+0122	S(?)	22h10m30.0s	+01d37m10s	0.0130	49	(63.5, −40.2)	98	$<0.2^c$	B95	—	—	—
						(58.8, −42.4)	189					
PKS 2201+044	BL	22h04m17.6s	+04d40m02s	0.0270	108	(63.5, −40.2)	109	530	W90	—	0.2^l	B94
NGC 7189	L	22h03m16.0s	+00d34m16s	0.0302	122	(63.5, −40.2)	151	13.0^c	C02	3.1	—	—
						(58.8, −42.4)	108					
NGC 1358	Sy2	03h33m39.7s	−05d05m22s	0.0134	54	(−170.6, −45.7)	51	8.7^c	C98	0.4	0.04	U05
						(−165.9, −46.9)	166					
Mrk 612	Sy2	03h30m40.9s	−03d08m16s	0.0205	83	(−170.6, −45.7)	81	5.1^c	C98	1.2	0.04	G05
NGC 1320	Sy2	03h24m48.7s	−03d02m32s	0.0089	35	(−170.6, −45.7)	130	3.3	G06	2.2	—	—
Mrk 609	Sy2	03h25m25.3s	−06d08m38s	0.0345	143	(−170.6, −45.7)	133	12.5^c	C98	2.6	—	—
						(−165.9, −46.9)	169					
KUG 0322-063	Sy1	03h25m11.6s	−06d10m51s	0.0338	140	(−170.6, −45.7)	137	11.3^c	C98	2.1	—	—
						(−165.9, −46.9)	171					
NGC 1346	L(?)	03h30m13.3s	−05d32m36s	0.0135	54	(−165.9, −46.9)	152	10.4^c	C98	3.1	—	—
NGC 7626	L	23h20m42.5s	+08d13m01s	0.0114	42	(88.8, −47.1)	86	210	W90	—	0.03^l	T05
2MASX J2327	Sy2	23h27m42.6s	+08d45m30s	0.0294	118	(88.8, −47.1)	122	$<0.5^c$	C98	—	—	—
NGC 7674	Sy2	23h27m56.7s	+08d46m45s	0.0289	116	(88.8, −47.1)	125	90.6^c	C02	5.6	0.05	L04
NGC 7591	L	23h18m16.3s	+06d35m09s	0.0165	64	(88.8, −47.1)	186	21.4^c	C02	7.2	—	—
NGC 7130	Sy2	21h48m19.5s	−34d57m05s	0.0161	64	(12.1, −49.0)	117	63.3^c	M03	16	0.006	Gm06
NGC 7135	L(?)	21h49m46.0s	−34d52m35s	0.0088	33	(12.1, −49.0)	126	2.3^c	C98	0.2	—	—
6dF J2132022	Sy1	21h32m02.2s	−33d42m54s	0.0293	120	(12.1, −49.0)	127	1.1^c	C98	—	—	—
NGC 1204	L	03h04m39.9s	−12d20m29s	0.0143	57	(−163.8, −54.4)	96	9.4^c	C90	7.8	—	—
MCG-02-08-039	Sy2	03h00m30.6s	−11d24m57s	0.0299	123	(−163.8, −54.4)	174	3.6^c	C98	0.5	—	—
ESO 404-IG042	S2	22h13m17.5s	−37d00m58s	0.0340	140	(4.2, −54.9)	76	2.2^c	C98	0.7	—	—
PKS 2158-380	FR II	22h01m17.1s	−37d46m24s	0.0333	137	(4.2, −54.9)	126	590	W90	0.3	—	—
IC 5169	Sy2	22h10m10.0s	−36d05m19s	0.0104	39	(4.2, −54.9)	131	8.3^c	M03	3.4	—	—
NGC 0424	Sy1	01h11m27.6s	−38d05m00s	0.0118	46	(−75.6, −78.6)	25	9.6^c	C98	1.8	0.1	U05
ESO 351-G025	Sy2	00h58m22.3s	−36d39m37s	0.0346	143	(−75.6, −78.6)	153	2.4^c	C98	—	—	—
ESO 352-G048	Sy2	01h20m54.7s	−36d19m26s	0.0322	132	(−75.6, −78.6)	163	$<0.5^c$	C98	—	—	—

REFERENCES. — (B95) Becker et al. 1995; (B06) Beckmann et al. 2006; (B07) Bird et al. 2007; (B99) Bock et al. 1999; (B94) Brinkmann et al. 1994; (C90) Condon et al. 1990; (C98) Condon et al. 1998; (C02) Condon et al. 2002; (G06) Gallimore et al. 2006; (Gm06) González-Martín et al. 2006; (G94) Gregory et al. 1994; (G05) Guainazzi et al. 2005; (L04) Lutz et al. 2004; (M05) Marshall et al. 2005; (M03) Mauch et al. 2003; (M92) Mollenhoff et al. 1992; (S89) Sadler et al. 1989; (S06) Shinozaki et al. 2006; (T05) Tajer et al. 2005; (U05) Ueda et al. 2005; (W92) White & Becker 1992; (W90) Wright & Otrupcek 1990.

NOTE. — [1] Name of the source. [2] AGN classification (Sy1/Sy2: Seyfert galaxy of the type 1/type 2; L: LINER; FR I: radio galaxy of the FR I type; BL: BL Lacertae object). [3-4] Equatorial coordiantes (J2000.0). [5] Redshift of the source. [6] Luminosity distance for the assumed cosmology ($H_0 = 73\,{\rm km\,s^{-1}\,Mpc^{-1}}$, $\Omega_{\rm M} = 0.27$, $\Omega_\Lambda = 0.73$) except for NGC 5128 (Cen A) and NGC 4945, where the distances are known (Karachentsev et al. 2007). [7] Galactic coordiantes for the nearby UHECR event. [8] Separation between an AGN and a nearby UHECR event. [9] The total 5 GHz flux in mJy units (^{c}fluxes converted from the ones provided at lower frequencies assuming radio spectral index $\alpha = 0.7$). [10] References for column 9. [11] The total 60 μm flux in Jy units from the IRAS survey (Moshir et al. 1990). [12] The total observed $2 - 10$ keV flux in $\times 10^{-11}$ erg cm^{-2} s^{-1} units (^{l}fluxes provided at lower photon energy range: $0.5 - 7$ keV in Marshall et al. (2005), or $0.1 - 2.0$ keV in Brinkmann et al. (1994) and Tajer et al. (2005); ^{h}fluxes converted from the ones provided at higher photon energy range $40 - 100$ keV in Bird et al. (2007), assuming X-ray photon index $\Gamma_X = 2.0$). [13] References for column 12.